

## Article

# Semitransparent Decorative Coatings Based on Optical Interference of Metallic and Dielectric Thin Films for High Temperature Applications

Enrique Carretero \* and Rafael Alonso

Applied Physics Department, University of Zaragoza, C/Pedro Cerbuna, 12, 50009 Zaragoza, Spain; ralonso@unizar.es

\* Correspondence: ecarre@unizar.es; Tel.: +34-876-553-769

Received: 12 April 2018; Accepted: 9 May 2018; Published: 11 May 2018



**Abstract:** This paper introduces a thin film multilayer structure composed of dielectric and metallic layers that allows for a wide range of aesthetic appearances using the phenomenon of optical interference. In addition, this multilayer structure allows the reflection and transmission coefficients to be controlled independently. The application of these decorative coatings to induction stoves is also studied. The aim is to provide an attractive aesthetic appearance for the transparent glass-ceramic, and allow the visualization of blue and white lighting systems. Moreover, degradation of these decorative coatings is studied at high temperatures, so as to ensure that the coating does not change its aesthetic appearance during normal operation of the stove. It has been found to be necessary to use dielectric materials with low diffusion coefficients of oxygen, or not containing oxygen, to prevent oxidation of the metal layers when subjecting the coating to high temperatures.

**Keywords:** decorative coatings; DC pulsed magnetron sputtering; optical interference; thin films; induction cookers

## 1. Introduction

Nowadays, the aesthetic appearance of consumer products has gained special importance, being one of the most decisive factors affecting purchasing decisions. Therefore, research into decorative coatings is of considerable commercial interest.

Semitransparent coatings are required for the control of the optical transmittance of a surface. For example, users may wish to see a TFT (Thin Film Transistor) display screen while an appliance is switched on, but not while it is turned off. In this case, a compromise has been found. The coating must have sufficient transmittance to allow perfect visualization of lighting devices and be absorbent enough to hide such devices when they are turned off, resulting in a more homogeneous, uniform, and aesthetically-pleasing surface. The ideal transmittance values for such applications are between 1% and 4% when LEDs (Light Emitting Diodes) are used as lighting systems. When it is required to view the TFT screens, the transmittance coating must be higher to compensate for the lower brightness of these screens. In this case, the ideal values are usually between 10% and 15%.

The aesthetic appearance of coatings is determined by the reflection coefficients of the coating, and can be described by color coordinates. Interferential optical coatings allow reflectance and transmittance curves to be adjusted with great freedom, depending on the multilayer structure used [1–4].

A very important field of application is the use of these decorative coatings in transparent glass-ceramic cookers [5–7]. Glass-ceramics currently found on the market can be classified into two types according to their optical properties. The first is black glass-ceramic “in bulk”, which is black in color

and has very low transmittance values for wavelengths lower than 550 nm, so that lighting and signaling blue are greatly attenuated (see, for example, Schott CERAN Hightrans, SCHOTT AG, Mainz, Germany). The second is transparent glass-ceramic, which has very similar mechanical, electrical, and thermal properties, but has a transmittance of about 80% in the visible region of the spectrum (Schott CERAN Cleartrans). Transparent glass-ceramic requires a coating to give it a particular aesthetic appearance and to control the transmittance values in the visible spectrum, see Figure 1.

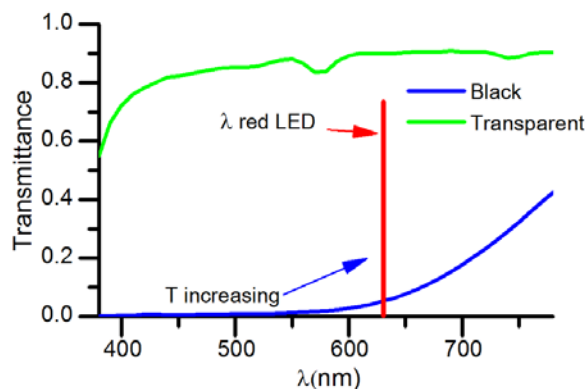


**Figure 1.** Optical transmittance of black and transparent ceramic glass (Schott CERAN HightransEco and Cleartrans).

Thin film decorative coatings can be obtained in two very different ways. The first is searching for materials having the desired optical properties, such as the deposition of TiN or ZrN to reproduce the aesthetic appearance of gold [8–10], the deposition of metal oxynitrides [11,12], or the deposition of alloys having optical properties that comply with the requirements [13–15]. This method entails a laborious search for materials with the required optical properties, and a calibration of the deposition conditions of these materials, because their optical properties are often dependent on the reactive gas flow during the deposition process. Moreover, such properties may be substantially affected by small sources of contamination, since the deposition of these materials is usually carried out in the vicinity of the “transition mode” where a small change in the deposition conditions may mean a big change in the properties of the film. This causes great inconvenience in terms of repeatability of the process. Another strategy that can be followed is the development of interferential decorative coatings based on the interference of different amplitudes reflected in each of the interfaces of the multilayer. Using this phenomenon, the transmission and reflection spectrum can be controlled depending on the multilayer structure [16,17], determined by the complex refractive indexes of each layer (given by the deposited material) and their thicknesses [1,3].

Interferential optical coatings have been the subject of much study, and are the basis for the development of optical filters and anti-reflective coatings. These applications typically use only dielectric layers with low optical absorption, so that the optical absorption of the coating is negligible, and transmission and reflection spectra are complementary. Moreover, if metal layers with optical absorption are also used, it is possible to control the optical absorption of the coating. Thus, it is possible to modify the value of the optical transmittance without changing the reflection value, so that there is some independence between these values [18,19].

In addition to having certain optical properties, the coating should withstand exposure to the high temperatures reached with induction stoves (above 400 °C) without the optical properties of the coating being altered to such a degree that a change in the coating color can be visually detected [20,21].

The final objective of this work is to develop coatings with different aesthetic aspects. In addition, these coatings must be semitransparent and allow a good visualization of light sources (LEDs, screens) without changing their chromaticity. On the other hand, the coatings must also withstand the high temperatures that are reached in induction cookers during their use. This type of coating would be

a great advance, since ceramic glasses currently change the chromaticity of light sources, and the available coatings do not have the necessary optical properties.

## 2. Materials and Methods

Stainless steel (Sst),  $\text{SiAlN}_x$ , and  $\text{SnO}_2$  thin films were deposited in a semi-industrial high vacuum magnetron sputtering system by the DC pulsed technique, using rectangular 600 mm  $\times$  100 mm targets having a 12 mm thickness. The substrates were ceramic glass pieces of 300 mm  $\times$  260 mm and 4 mm thick. The thickness of the deposited layers had a good homogeneity, achieved by using an in-line deposition system and a very large magnetron. The ceramic glass had a low thermal expansion coefficient, making it resistant to large temperature gradients without breaking. Prior to deposition, the substrate was cleaned with a detergent solution (ACEDET 5509, Aachener Chemische Werke, Rostocker, Germany) and finally rinsed with distilled water. The deposition system and the process are similar to those used in [12,22,23].

Multilayer coatings were grown with a base pressure of  $2.0 \times 10^{-4}$  Pa, and a working pressure in the range of  $10^{-1}$  Pa. Ar and  $\text{N}_2$  (99.99%) flows were introduced into the process chamber and controlled via mass flow controllers. The substrate was maintained at room temperature during deposition. Sst films were deposited from a Sst 316 (99.99%) target. The Ar flow was fixed at 200 sccm (standard cubic centimeters per minute), and the power applied was 2000 W, equivalent to a power density of  $3.33 \text{ W/cm}^2$ .  $\text{SiAlN}_x$  was deposited by reactive sputtering from a SiAl target (90% Si and 10% Al, 99.99% pure). The Ar flow was fixed at 100 sccm, and the  $\text{N}_2$  flow at 100 sccm. The power applied was 2500 W, equivalent to a power density of  $4.17 \text{ W/cm}^2$ .  $\text{SnO}_2$  was deposited by reactive sputtering from a Sn target (99.99% pure). The Ar flow was fixed at 100 sccm and the  $\text{O}_2$  flow at 180 sccm. The power applied was 1800 W, equivalent to a power density of  $3.00 \text{ W/cm}^2$ . These deposition conditions are similar to those used in [23].

The sputtering rate was calibrated by individually depositing a film of every used material and measuring its thickness by mechanical profilometry with a DekTak XT equipment (Bruker, Billerica, MA, USA), which has a vertical resolution of 0.1 nm, and whose typical error is approximately 1 nm.

The layers were deposited sequentially to form a multilayer of five layers made up of substrate/dielectric/Sst/dielectric/Sst/dielectric with the dielectric being  $\text{SiAlN}_x$  or  $\text{SnO}_2$ . The thicknesses of each of the layers may vary according to the aesthetic appearance to be obtained.

Specular transmittance and reflectance measurements were performed with a spectrophotometer in the visible region of the electromagnetic spectrum, between 380 nm and 780 nm with 10 nm intervals, at an angle of incidence of  $8^\circ$ .

Complex refractive indexes are calculated from spectrophotometric measurements and the thickness of the films [24–26]. For this reason, each material is deposited individually on a known glass substrate. In the case of dielectric materials, we fit the results by means of the Sellmeier equation.

The transmission and reflection coefficients of a multilayer structure can be calculated by any formalism used in the theory of interferential multilayers. This formalism relates the amplitude of the electromagnetic field at both sides of the multilayer structure by means of a  $2 \times 2$  matrix, from which the transmission and reflection coefficients can be determined. Thus, it is only necessary to know the thicknesses and the complex refractive indexes of the layers forming the multilayer [1,2,27].

To determine the resistance to temperature, a so-called “abandonment test” was carried out (see Figure 2). This test is commonly used by developers in cooker quality tests. Starting from thermal equilibrium, a ferromagnetic disc is heated for 15 min at maximum power. We have determined that the effect of this test produced on the sample is similar to placing the sample in an oven at  $400^\circ\text{C}$  for 15 min.



**Figure 2.** Abandonment test on induction hob with green decorative coating.

### 3. Results and Discussion

Interferential decorative coatings made up of multilayer structures formed by 5 alternate layers of dielectric and metal materials were deposited. Although in some cases it is possible to use three layers, the 5-layer structure allows a better adjustment of the optical properties of the coating. This is of particular interest for obtaining a black coating color to reproduce the aesthetic appearance of black glass-ceramic. In [28], a coating with a similar multilayer structure for a black coating in reflection on the coating/air face was described. In [28], the coating was opaque, while in the present work, the multilayer structure is adapted for a black coating (and other colors) on the glass-ceramic/coating face, which at the same time is designed to be semitransparent.

There is a compromise between the aesthetic possibilities and the number of layers required. It is therefore desirable to define a layered structure that is not very large, but allows a wide range of aesthetic appearances to be obtained, including the color black (low reflectance), which are essential for induction stoves. It was therefore decided that a structure of 5 layers (3 dielectric and 2 metallic) would offer a wide range of possibilities (see Figure 3). The layers have different functions in adjusting the optical properties of the coating:

- 1st Layer (transparent dielectric): this layer may have thicknesses between 0 nm and 60 nm, although in some cases, it may be omitted completely, this possibility is limited by the use of some materials with determined refractive indexes, which is a very limited possibility. Generally, this layer is deposited in order to have more degrees of freedom when adjusting the reflection spectrum, so that the desired reflectance curves can be more easily achieved.
- 2nd Layer (absorbent metal): this layer has a 7–10 nm thickness. The layer must be thin so that the reflected intensities in the lower interfaces are not strongly attenuated. These intensities must have sufficient amplitude to significantly affect the result of the interference of the reflected waves. A change in the thickness of this layer greatly affects optical reflectance [28].
- 3rd Layer (transparent dielectric): the function of this layer is to generate more interfaces, thereby increasing the degrees of freedom when adjusting the reflectance curves.
- 4th Layer (absorbent metal): the thickness of this layer is usually between 20 nm and 50 nm. The function of this layer is essentially the selection of the transmission of the coating by adjusting its thickness due to absorption of the chosen material. It allows adjustment of the said transmittance values by less than 20%, since for larger values of transmittance, it is difficult to isolate the change in the reflection coefficients of changes in transmission.
- 5th Layer (transparent dielectric): the thickness of this layer will vary between 40 nm and 50 nm. This layer hardly affects the reflection values for the glass face because it is below the absorbing metallic layers, thereby, the reflected intensities in their interfaces will be very attenuated. Its function is to protect the metal layer from atmospheric oxygen that can oxidize it and to provide the coating with greater mechanical strength.

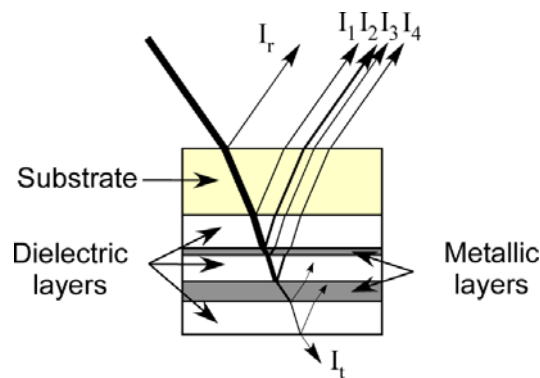


**Figure 3.** Multilayer structure of decorative coatings.

Figure 4 shows different aesthetic appearances obtained from the five-layer structure after performing the “abandonment test” on these samples. Figure 4a shows a coating compound of  $\text{SnO}_2$  and Sst layers where the optical properties have changed considerably in the area of coating where the “abandonment test” was performed. Figure 4b shows another sample of black/navy blue coating, composed of layers of  $\text{SiAlN}_x$  and Sst that have hardly been affected by being exposed to the “abandonment test”. Figure 4c,d show other coatings with different aesthetic appearances based on  $\text{SiAlN}_x$  and Sst layers that did not suffer any appreciable change in their optical properties when exposed to the “abandonment test”.

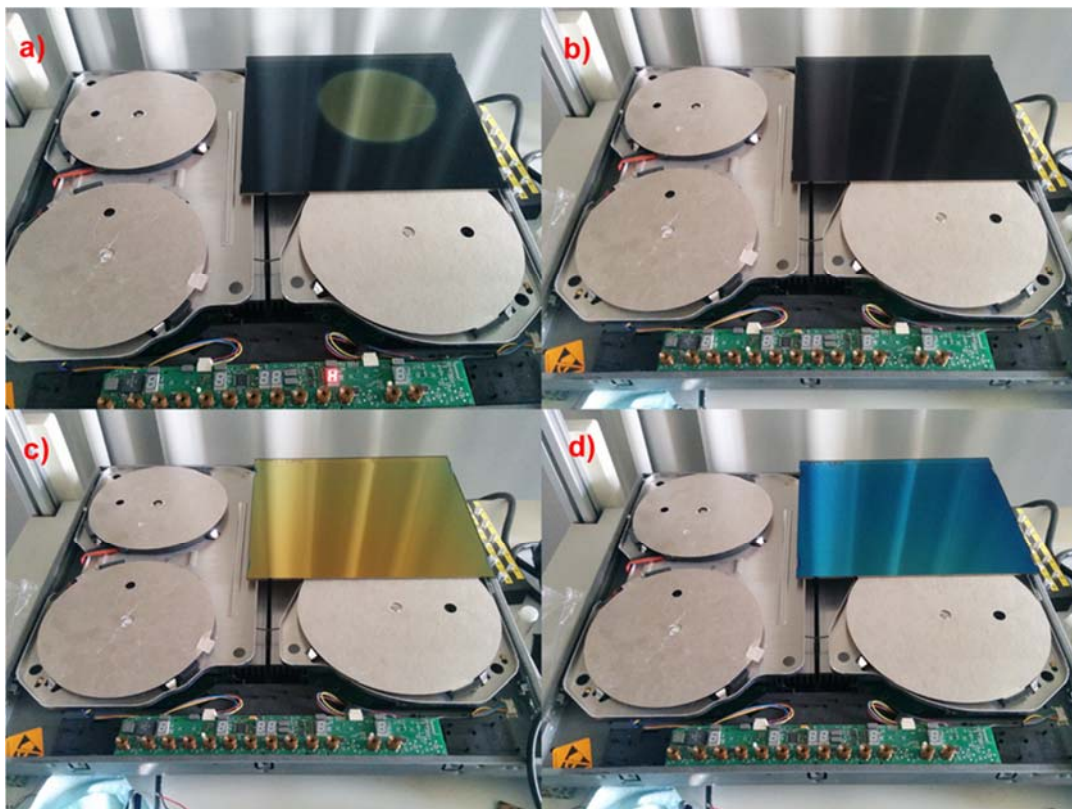


**Figure 4.** Some decorative coatings after abandonment test: (a) Navy/black coating with  $\text{SnO}_2$  and Sst layers; (b) Navy/black coating with  $\text{SiAlN}_x$  and Sst layers; (c) Yellow coating with  $\text{SiAlN}_x$  and Sst layers; and (d) Sky blue coating with  $\text{SiAlN}_x$  and Sst layers.



Figure 5 shows reflection spectra of various deposited multilayers (see Table 1). A correspondence between the experimental values and the simulated data using can be observed using the matrix method based on the continuity of the tangential components of electromagnetic fields. The complex refractive indexes of the deposited materials are presented in the Supplementary Material. The refractive indices of  $\text{SiAlN}_x$  and  $\text{SnO}_2$  are very close. Therefore, these materials can be interchangeable without showing appreciable changes in the optical properties of the coating (using the same thicknesses, see Table 1).

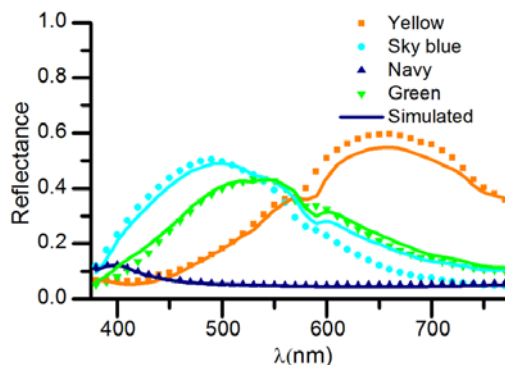


**Figure 5.** Reflectance of some decorative coatings. Experimental data (points) and simulated data (lines).

**Table 1.** Film thicknesses (in nm) for coatings with different aesthetic appearances.

Film	Green	Yellow	Sky Blue	Navy/Black
$\text{SnO}_2$ or $\text{SiAlN}_x$	30	21	9	50
Sst	9	10	9	9
$\text{SnO}_2$ or $\text{SiAlN}_x$	106	140	100	66
Sst	42	43	47	45
$\text{SnO}_2$ or $\text{SiAlN}_x$	41	48	47	47

Resistance to the abandonment test was checked for all coatings, both in the case where  $\text{SnO}_2$  is used as the dielectric material and in the case of  $\text{SiAlN}_x$ . In the case of coatings composed of  $\text{SnO}_2$  layers, the effect of the abandonment test considerably degraded the optical properties of the coating, resulting in a clearly distinguishable aesthetic appearance in the area exposed to high temperature (Figure 4a), leading to a great change in the transmission and reflection spectra of the coating (Figure 6). A quantitative value of the change in the aesthetic appearance can be obtained from the difference in the color coordinates. Thus, using the color coordinate system CIELAB 1976 described in chapters 7 and 8 in [29], and using the color difference parameter,

$$\Delta E = \sqrt{(\Delta L)^2 + (\Delta a)^2 + (\Delta b)^2} \quad (1)$$

A value of  $\Delta E_{ref} = 32.1$  was obtained for the color change in reflection and  $\Delta E_{trans} = 24.4$  for the color change in transmission. The change of the optical properties of the coating is due to the diffusion of oxygen in each  $\text{SnO}_2$ /Sst interface. The dynamic of the oxidation in these interfaces was studied in [22,23]. Thus, the reflection and transmission coefficients after the abandonment test can be adjusted using the multilayer model in the interface used in [23] and the refractive indexes measured for the stainless steel oxide with different compositions. In particular, we used the refractive indexes of stainless steel oxide with 19% and 29% of oxygen by weight, given in [12]. In this case, only two intermediate layers of stainless steel oxide are required in each  $\text{SnO}_2$ /Sst interface, instead of three intermediate layers, as in [12], because the thicknesses of the metal layers, in this case, are small. Table 2 shows the simulated multilayer that better adjusts the transmission and reflection spectra of the coating after having been subjected to the “abandonment test” (see Figure 6). In this case, although the deposited multilayer is the same as that described in Table 1, exposure to high temperatures oxidizes

the Sst forming intermediate layers of  $\text{SstO}_x$ . Given this effect, it is desirable to use materials in the dielectric layers not containing oxygen, such as  $\text{Si}_3\text{N}_4$ ,  $\text{AlN}$ , or  $\text{SiAlN}_x$ ; or materials having a high affinity for oxygen, but which have a low coefficient of diffusion of oxygen, such as  $\text{Al}_2\text{O}_3$ .

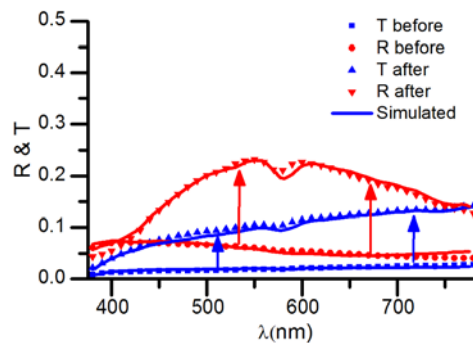


**Figure 6.** Effect of abandonment test on transmittance and reflectance spectra of navy/black coatings with  $\text{SnO}_2$  and Sst layers. Experimental data (points) and simulated data (lines).

**Table 2.** Film thicknesses (in nm) for simulated multilayer of  $\text{SnO}_2$ /Sst after the abandonment test.

N° Film	Material	Thickness (nm)
1	$\text{SnO}_2$	50
2	$\text{SstO}_x$ (29% Oxygen)	4
3	$\text{SstO}_x$ (19% Oxygen)	1.7
4	Sst	1
5	$\text{SstO}_x$ (19% Oxygen)	1.7
6	$\text{SstO}_x$ (29% Oxygen)	4
7	$\text{SnO}_2$	49
8	$\text{SstO}_x$ (29% Oxygen)	6
9	$\text{SstO}_x$ (19% Oxygen)	2.5
10	Sst	23
11	$\text{SstO}_x$ (19% Oxygen)	2.5
12	$\text{SstO}_x$ (29% Oxygen)	6
13	$\text{SnO}_2$	49

On the other hand, if  $\text{SiAlN}_x$  layers are used as dielectric material, it is demonstrated that the abandonment test modifies the transmittance and reflectance curves to a lesser degree. Figure 7 shows that the experimental points of reflectance and transmittance before and after the abandonment test are superimposed.

No color change can be observed (see Figure 4b,d), and quantifying the color difference gives  $\Delta E_{ref} = 1.3$  (reflection color change) and  $\Delta E_{trans} = 1.2$  (transmission color change). This color change is very small. Moreover, if a second abandonment test is performed, it is observed that the color change in the test is even smaller, since the layer is more stabilized after the first abandonment test.

The transmittance of the developed coatings has great advantages over current glass-ceramics, because it has a uniform transmittance of about 2% in the visible region of the spectrum. Furthermore, the values of the reflectance of the black/navy coating approach the value of 4% which current glass-ceramics have, and these can be adjusted even better with small changes in the design of the multilayer.

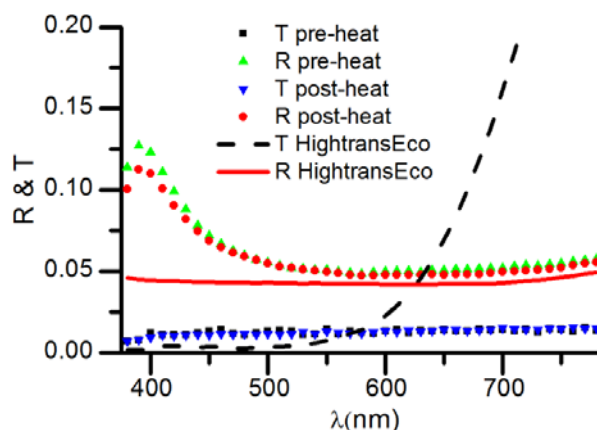


**Figure 7.** Effect of abandonment test on transmittance and reflectance spectra of navy/black coatings with  $\text{SiAlN}_x$  and Sst layers. Experimental data of coatings (points) and Schott Ceran HightransEco (lines).

Figure 8 shows a photograph of several coatings with the same multilayer structure as that presented in this work. White LEDs can be seen without changing the original chromaticity of the light sources, unlike in the case of black glass-ceramic (Schott CERAN HightransEco). Thus, it is evident that the use of these coatings improves the visualization of the light sources located inside the stove. The manufacturing of these coatings at industrial level is perfectly viable, because the sputtering is scalable. In addition, it allows the adjustment of the coating optical properties of the coating in a simple way by changing only the thickness of the layers. This point is very important because it can provide a differentiation of product and could respond to the demand for products which can be customized by users.

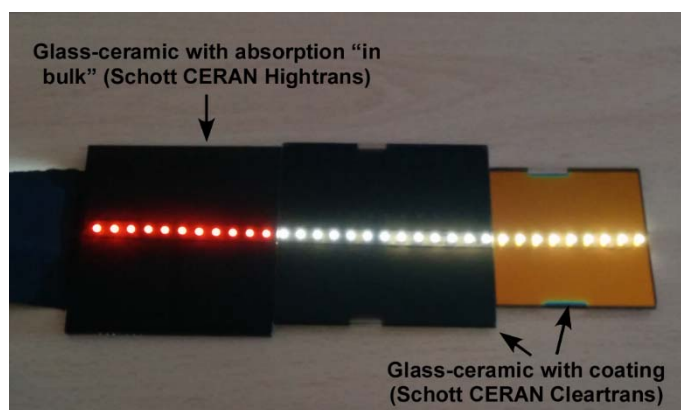


**Figure 8.** Visualization of white LEDs across black glass-ceramic (left) and different transparent glass-ceramics with semitransparent decorative coatings: navy/black (center) and yellow (right).

#### 4. Conclusions

The versatility has been demonstrated of a 5-layer structure composed of dielectric and metal materials that allows the selection between many different aesthetic appearances in reflection. In particular, black coatings with low reflectance have been achieved, reproducing the actual aesthetic appearance of the glass-ceramic with absorption in bulk. In addition, these coatings allow the transmittance of the coating to be selected by adjusting the thickness of the metal layers without the reflection values being greatly affected. On the other hand, it has been found necessary to use dielectric materials with low diffusion coefficients of oxygen, or not containing oxygen, to prevent oxidation of the metal layers when subjecting the coating to high temperatures that can be achieved



in induction cookers or other applications. This phenomenon can greatly alter the optical properties of the coatings, as it modifies the effective thicknesses and refractive indexes of the metal layers. Finally, good color reproduction in the transmission of the coatings developed in this work has been demonstrated compared with black glass-ceramic, so that blue or white LEDs can be visualized without their look being attenuated or their chromaticity altered.

## 5. Patents

The results of this work have given rise to two patents [6,7].

**Supplementary Materials:** The following are available online at <http://www.mdpi.com/2079-6412/8/5/183/s1>, Figure S1: Complex refractive indexes of Sst, Figure S2: Refractive indexes of  $\text{SiAlN}_x$ , Figure S3: Refractive indexes of  $\text{SnO}_2$ .

**Author Contributions:** E.C. and R.A. conceived and designed the experiments; E.C. performed the experiments; E.C. and R.A. analyzed the data; E.C. wrote the paper.

**Funding:** This research was partly funded by Spanish Ministerio de Economía y Competitividad (RTC-2014-1847-6), in part by the Diputación General de Aragón/FEDER through the funding for the Photonics Technologies Group (GTF), in part by the Diputación General de Aragón under FPI programme (B143/12) and in part by the BSH Home Appliances Group.

**Acknowledgments:** We thank Carmen Cosculluela for her valuable help.

**Conflicts of Interest:** The authors declare no conflict of interest.

## References

- Thelen, A. *Design of Optical Interference Coatings*; McGraw-Hill: New York, NY, USA, 1989; ISBN 978-0-07-063786-3.
- Dobrowolski, J.A. Dobrowolski optical properties of films and coatings. In *Handbook of Optics*; McGraw-Hill: New York, NY, USA, 1995; Volume I.
- Macleod, H.A. *Thin-Film Optical Filters*, 4th ed.; CRC Press: Boca Raton, FL, USA, 2010; ISBN 978-1-42-007303-4.
- Gläser, H.J. *Large Area Coating*; Von Ardenne Anlagentechnik GmbH: Dresden, Germany, 2000.
- Garcia, J.R.; Villuendas, F.; Alonso, R.; Subias, J.M.; Pelayo, F.J.; Buñuel, M.A.; Planas, F.; Ester, F.J.; Perez, P.; Sancho, D. Placa de Cubierta de Aparato Domestico con una Placa de Soporte al Menos Semitransparente, Aparato Domestico Para Preparar Alimentos, y Procedimientos Para Fabricar una Placa de Cubierta de Aparato Domestico. P200931263, February 2013.
- Esteban, R.A.; Magdalena, M.A.B.; Chamarro, E.C.; Sola, F.J.E.; Zueco, F.J.P.; Cabeza, P.P.; Layunta, F.P.; Domingo, J.M.S.; Yuste, F.V. Hot Plate and Hob Comprising a Corresponding Hot Plate. U.S. Patent 14/007,727, 20 March 2014.
- Esteban, R.A.; Magdalena, M.A.B.; Chamarro, E.C.; Sola, F.J.E.; Zueco, F.J.P.; Cabeza, P.P.; Layunta, F.P.; Domingo, J.M.S.; Yuste, F.V. Hot Plate Comprising a Coating Applied to the Lower Side Thereof. U.S. Patent 14/007,725, 17 July 2014.
- Chandra, R.; Chawla, A.K.; Kaur, D.; Ayyub, P. Structural, optical and electronic properties of nanocrystalline TiN films. *Nanotechnology* **2005**, *16*, 3053. [CrossRef]
- Yuste, M.; Escobar Galindo, R.; Carvalho, S.; Albella, J.M.; Sanchez, O. Improving the visible transmittance of low-e titanium nitride based coatings for solar thermal applications. *Appl. Surf. Sci.* **2011**, *258*, 1784–1788. [CrossRef]
- Niyomsoan, S.; Grant, W.; Olson, D.L.; Mishra, B. Variation of color in titanium and zirconium nitride decorative thin films. *Thin Solid Films* **2002**, *415*, 187–194. [CrossRef]
- Carvalho, P.; Borges, J.; Rodrigues, M.S.; Barradas, N.P.; Alves, E.; Espinós, J.P.; González-Elipe, A.R.; Cunha, L.; Marques, L.; Vasilevskiy, M.I.; et al. Optical properties of zirconium oxynitride films: The effect of composition, electronic and crystalline structures. *Appl. Surf. Sci.* **2015**, *358*, 660–669. [CrossRef]
- Carretero, E.; Alonso, R.; Pelayo, C. Optical and electrical properties of stainless steel oxynitride thin films deposited in an in-line sputtering system. *Appl. Surf. Sci.* **2016**, *379*, 249–258. [CrossRef]
- Garcia-Garcia, F.J.; Gil-Rostra, J.; Yubero, F.; Gonzalez-Elipe, A.R. Electrochromism in  $\text{WO}_x$  and  $\text{W}_x\text{Si}_y\text{O}_z$  thin films prepared by magnetron sputtering at glancing angles. *Nanosci. Nanotechnol. Lett.* **2013**, *5*, 89–93. [CrossRef]

14. Gil-Rostra, J.; Garcia-Garcia, F.; Yubero, F.; Gonzalez-Elipe, A.R. Tuning the transmittance and the electrochromic behavior of  $\text{Co}_x\text{Si}_y\text{O}_z$  thin films prepared by magnetron sputtering at glancing angle. *Sol. Energy Mater. Sol. Cells* **2014**, *123*, 130–138. [[CrossRef](#)]
15. Figueiredo, N.M.; Vaz, F.; Cunha, L.; Pei, Y.T.; De Hosson, J.T.M.; Cavaleiro, A. Optical and microstructural properties of Au alloyed Al–O sputter deposited coatings. *Thin Solid Films* **2016**, *598*, 65–71. [[CrossRef](#)]
16. Kats, M.A.; Blanchard, R.; Genevet, P.; Capasso, F. Nanometre optical coatings based on strong interference effects in highly absorbing media. *Nat. Mater.* **2013**, *12*, 20–24. [[CrossRef](#)] [[PubMed](#)]
17. Panjan, M.; Klanjšek Gunde, M.; Panjan, P.; Čekada, M. Designing the color of AlTiN hard coating through interference effect. *Surf. Coat. Technol.* **2014**, *254*, 65–72. [[CrossRef](#)]
18. Sullivan, B.; Byrt, K. Metal/Dielectric Transmission Interference Filters with Low Reflectance. 2. Experimental Results. *Appl. Opt.* **1995**, *34*, 5684–5694. [[CrossRef](#)] [[PubMed](#)]
19. Ma, P.; Lin, F.; Dobrowolski, J.A. Design and manufacture of metal/dielectric long-wavelength cutoff filters. *Appl. Opt.* **2011**, *50*, C201–C209. [[CrossRef](#)] [[PubMed](#)]
20. Macadam, D. Uniform Color Scales. *J. Opt. Soc. Am.* **1974**, *64*, 1691–1702. [[CrossRef](#)] [[PubMed](#)]
21. MacAdam, D.L. Visual sensitivities to color differences in daylight. *J. Opt. Soc. Am.* **1942**, *32*, 247–274. [[CrossRef](#)]
22. Carretero, E.; Alonso, R.; Marco, J.M. Oxygen diffusion at high temperatures within the  $\text{SnO}_2/\text{Sst}$  interlayer in sputtered thin films. *Appl. Surf. Sci.* **2015**, *359*, 669–675. [[CrossRef](#)]
23. Carretero, E.; Alonso, R.; Pelayo, C. Determination of oxygen diffusion in the  $\text{SnO}_2/\text{stainless steel}$  interface of thin films by spectrophotometric measurements. *J. Phys. Appl. Phys.* **2016**, *49*, 215302. [[CrossRef](#)]
24. Case, W. Algebraic-Method for Extracting Thin-Film Optical-Parameters from Spectrophotometer Measurements. *Appl. Opt.* **1983**, *22*, 1832–1836. [[CrossRef](#)] [[PubMed](#)]
25. Panayotov, V.; Konstantinov, I. Determination of Thin-Film Optical-Parameters from Photometric Measurements—An Algebraic-Solution for the  $(t, R_t, R_b)$  Method. *Appl. Opt.* **1991**, *30*, 2795–2800. [[CrossRef](#)] [[PubMed](#)]
26. Bennett, J.; Booty, M. Computational Method for Determining N and K for Thin Film from Measured Reflectance Transmittance and Film Thickness. *Appl. Opt.* **1966**, *5*, 41–43. [[CrossRef](#)] [[PubMed](#)]
27. Marco, J.M.; Uliaque, L.; Villuendas, F. Design and manufacture of solar control coatings for its application in laminated glass. *Bol. Soc. Esp. Ceram. Vidrio* **2001**, *40*, 113–118. [[CrossRef](#)]
28. Cho, S.-H.; Seo, M.-K.; Kang, J.-H.; Yang, J.-K.; Kang, S.-Y.; Lee, Y.-H.; Hwang, K.H.; Lee, B.D.; Lee, J.-G.; Song, Y.-W.; et al. A Black Metal-dielectric Thin Film for High-contrast Displays. *J. Korean Phys. Soc.* **2009**, *55*, 501–507. [[CrossRef](#)]
29. International Commission on Illumination. CIE 015:2004—*Colorimetry*, 3rd ed.; CIE: Vienna, Austria, 2004; ISBN 3-901-906-33-9.



© 2018 by the authors. Licensee MDPI, Basel, Switzerland. This article is an open access article distributed under the terms and conditions of the Creative Commons Attribution (CC BY) license (<http://creativecommons.org/licenses/by/4.0/>).